HHS Public Access

Author manuscript

Immunobiology. Author manuscript; available in PMC 2017 September 23.

Published in final edited form as:

Immunobiology. 2017 July ; 222(7): 831–841. doi:10.1016/j.imbio.2017.03.002.

The protection role of Atg16l1 in CD11c+ dendritic cells in murine colitis

Hong Zhang[a,b], **Libo Zheng**[a], **Jeremy Chen**[b], **Masayuki Fukata**[b], **Ryan Ichikawa**[b], **David Q. Shih**[b], and **Xiaolan Zhang**[a,*]

[a]Department of Gastroenterology, The Second Hospital of Hebei Medical University, Hebei, China

[b]F. Widjaja Foundation, Inflammatory Bowel & Immunobiology Research Institute, Cedars-Sinai Medical Center, Los Angeles, CA90048, USA

Abstract

The autophagy-related 16-like 1 gene (Atg16l1) is associated with inflammatory bowel disease (IBD) and has been shown to play an essential role in paneth cell function and intestinal homeostasis. However, the functional consequences of Atg16l1 deficiency in myeloid cells, particularly in dendritic cells (DCs), are not fully characterized. The aim of this study is to investigate the functional consequence of Atg16l1 in $CD11c^+$ DCs in murine colitis. We generated mice deficient in Atg16l1 in $CD11c^+$ DCs. Dextran Sulfate Sodium (DSS) and *S. typhimurium* infection induced colitis was used to assess the role of DCs specific Atg16l1 deficiency *in vivo* in murine colitis. Bone marrow derived dendritic cells (BMDC) were isolated and autophagy function was assessed with microtubule-associated protein 1 light chain 3β (Map1lc3b or LC3) by western blot. Uptake of Salmonella enteric serovar typhimurium (*S. typhimurium*) was assessed by flow cytometry and transmission electron microscopy (TEM). The production of reactive oxygen species (ROS) and intracellular *S. typhimurium* killing in BMDCs were assessed. We showed worsened colonic inflammation in Atg16l1 deficiency mice in DSS induced murine colitis with increased proinflammatory cytokines of IL-1β and TNF-α. Mechanistic studies performed in primary murine BMDCs showed that Atg16l1 deficiency increased ROS production, reduced microbial killing and impaired antigen processing for altered intracellular trafficking. Together, these results indicate impaired $CD11c^+$ DCs function with Atg16l1 deficiency contributes to the severity of murine colitis.

*Corresponding author at: Department of Gastroenterology, The Second Hospital of Hebei Medical University, 80 Huang He Street, Shijiazhuang, Hebei, 050000, China. xiaolanzh@126.com (X. Zhang).

Conflict of interest

The authors have declared that no conflict of interest exists.

Authors' contributions

David and Libo Zheng participated in the design of the study and performed the statistical analysis and drafted the manuscript. Hong Zhang collected data, analyzed histological scores and wrote the manuscript; Jeremy Chen did the Western blots; Ryan Ichikawa did the gentamycin protection assay, uptake assay and TEM work. Everyone in the group helped with the mouse sacrifice. Xiaolan Zhang participated in the design and coordination, helped to draft the manuscript and gave final approvals of the version to be published. All authors read and approved the final manuscript.

Appendix A. Supplementary data

Supplementary data associated with this article can be found, in the online version, at http://dx.doi.org/10.1016/j.imbio.2017.03.002.

Keywords

Inflammatory bowel disease; Autophagy; Atg16l1; Dendritic cells; ROS; IgA

1. Introduction

Autophagy remains one of the most interesting disease-specific revelations of inflammatory bowel disease (IBD) genetics with the discovery of risk variants in autophagy-related 16-like 1 gene (Atg16l1) and other autophagy genes (Györgyi et al., 2013). Autophagy represents a basic function of all the cells where cytosolic constituents are engulfed in a double-membrane vesicle and targeted for degradation by lysosomal fusion or is induced by the needs associated with metabolic changes such as starvation or the removal of microbes (xenophagy) (Congcong and Daniel, 2009). Autophagy is deeply implicated in the regulation of numerous physiologic functions including cell development and differentiation, survival and senescence, In regard to the immune system, autophagy affects fundamentally the inflammatory process and the innate and adaptive arms of immune responses, including clearance of intracellular bacteria, antigen presentation and the regulation of cytokines production and secretion (Györgyi et al., 2013; Salio et al., 2014).

Dendritic cells (DCs) are one of the antigen-presenting cells that bridge the innate and adaptive immune responses (Banchereau et al., 2000; Reise, 2006). Deregulation of DC function, either as a primary effect of gene mutations or as a consequence of defective integration with environmental cues, may result in intestinal disease (Rescigno and Di Sabatino, 2009). A recent study has shown that DCs from Crohn's disease (CD) patients carrying nucleotide binding oligomerization domain containing 2 (NOD2) or Atg16l1 risk variants were defective in autophagy induction, bacterial trafficking and antigen presentation as shown to inhibit major histocompatibility complex (MHC) II-mediated antigen presentation (Cooney et al., 2009). DC-specific deletion of an essential autophagy gene Atg5 made mice more susceptible to the infection of herpes simplex virus 2 due to the inability of DCs to present antigen and an appropriate $CD4^+$ T cell response (Lee et al., 2010). Autophagy in DCs was also found to be critical for an appropriate $CD4^+$ T cell responses against infection by respiratory syncytial virus (Reed et al., 2013).

The genome wide association studies (GWAS) have implicated autophagy-related proteins in human disease, including single-nucleotide polymorphisms in Atg16l1 that is associated with risk for IBD (Murthy et al., 2014). Published functional analyses demonstrated that the IBD associated single-nucleotide polymorphism (SNP), ATG16L1 T300A, is a loss-of-function SNP that leads to increased caspase-mediated cleavage of Atg16l1 protein, resulting in reduced autophagy (Lassen et al., 2014; Murthy et al., 2014; VanDussen et al., 2014). Cells from patients homozygous for the T300A variant, or epithelial cells transduced with this variant, fail to clear intracellular microbes indicating that reduced pathogen clearance in patients with this variant might contribute to risk of CD (Kuballa et al., 2008). Atg16l1 facilitates bacterial invasion and the ATG16L1 T300A variant reduces invasion of human cells by Salmonella (Jeannette et al., 2013). Mice lacking Atg16l1 in haematopoietic cells showed several features of dysfunctional immune homeostasis, including impaired

Paneth cell function and hypersecretion of IL-1β and IL-18 from macrophages following stimulation with lipopolysaccharide (LPS) (Saitoh et al., 2008). These observations are consistent with a role for autophagy in bacterial survival mechanisms, proinflammatory signaling and initiation of adaptive immune responses. And mice lacking Atg16l1 in epithelial cell exhibited Paneth cell abnormalities and were more susceptible to Salmonella infection whereas the phenotype of Atg16l1 deficiency in $CD11c^+$ DC was similar to WT mice (Conway et al., 2013). This suggested that although Atg16l1 in intestinal epithelial cells appears to be important for xenophagy and for maintaining gut homeostasis, it may be dispensable in CD11c+ DCs.

Additionally, given the importance of DCs in innate immune responses and autophagy for protection against active tuberculosis and pulmonary inflammation (Castillo et al., 2012), we generated mice with Atg16l1 deficiency in $CD11c^+$ DCs (Atg16l1ΔDC) by using Salmonella enteric serovar typhimurium (*S. typhimurium*) and Dextran Sulfate Sodium (DSS) as an independently colitis model, which showed worsened colonic inflammation and increased IL-1β and TNF-α in DSS-induced murine colitis models in mice with Atg16l1 deficiency in $CD11c^+$ DCs. Furthermore, Bone marrow-derived dendritic cells (BMDCs) were derived from Atg16l1 floxed ($Atg16l1^{f/f}$, controls) and Atg16l1 deficiency in $CD11c^+$ DCs (Atg16l1ΔDC) mice to explore the role of $CD11c^+$ DCs *in vitro*. As expectedly, Atg16l1 deficiency impaired the functions of primary BMDCs including increase in p40Phox and reactive oxygen species (ROS), decrease in intracellular *S. typhimurium* killing and shift of *S. typhimurium* to phagocytosis vesicles.

2. Materials & methods

2.1. Mice and generation of $Atg16l1^{f/f}$ mice

Cloning of *Atg16l1* targeting vector and generation of $Atg16l1^{f/f}$ mice were previously described (Zhang et al., 2017). To generate mice with conditional targeting of Atg16l1 specifically in dendritic cells, $Atg16l1^{f/f}$ mice were bred with mice expressing *cre* recombinase under the control of CD11c (CD11c-*cre*, Jax mice stock 007567) (Fig. 1A). For antigen presentation assay, OTII/RAGII mice (Taconic 1896) specific for $OVA_{323–339}$ were used. All mice were in C57BL/6J genetic background and were maintained under specific pathogen-free conditions in the Animal Facility at Cedars-Sinai Medical Center (CSMC). This study was carried out in strict accordance with the Guide for the Care and Use of Laboratory Animals of the National Institutes of Health. Animal studies were approved by the CSMC Animal Care and Use Committee (protocol 3723).

2.2. Induction of colitis, DAI and histopathological analysis

Protocol for *S. typhimurium* infection was performed as previously described with the following modification (Barthel et al., 2003). *S. typhimurium* 14028 (gift from Andreas Baumler, UC Davis) with Nalidixic acid resistance were grown in LB broth supplemented with Nalidixic acid (100 μg/ml) to OD 0.2–0.8. Mice pretreated with 20 mg of streptomycin (Sigma) were oral gavaged with 3×10^6 CFU of *S. typhimurium* and euthanized 5 days after infection. Acute DSS were performed by administration of DSS (40 000–50 000 MW; Merck Millipore) in drinking water for 7 days. Mice were sacrificed at day 7. chronic colitis

was induced by administration of 2.5% DSS (40 000–50 000 MW; Merck Millipore) in drinking water from day 1 to day 5, day 8 to day 12, day 15 to day 19 and day 22 to day 26 and distilled water during the remaining time. Mice were sacrificed at day 29. DAI was calculated as described (Barrett et al., 2012). Tissue samples were processed and stained with hematoxylin and eosin (H&E) by the CSMC Histology-Core. Histopathological scores were assigned in a blinded manner by two trained animal pathologists (DQS and HZ) using previously established scoring system for *S. typhimurium* (Barthel et al., 2003), acute DSS, and chronic DSS (Barrett et al., 2012).

2.3. Flow cytometry and IgA measurement

For flow cytometry, cells were acquired on a LSR II flow-cytometer (BD Biosciences, San Jose, CA) and analyzed using FlowJo analysis software. All the antibodies for the immune system were purchased from eBioscience. Live cells were selected using live/dead stain (Life Technologies), CD16/CD32 (clone 2.4G2) was used to block nonspecific FcR binding (eBiosciences). Fecal IgA flow cytometry was performed on two fecal pellets that were collected directly from 4 to 5 co-housed mice of the same genotype at 6–8 weeks of age. The fecal samples were homogenized in 1 mL phosphate buffered saline per 100 mg fecal material and centrifuged 50*g* for 15 min to remove large particles. Supernatants were stained for IgA by flow cytometry as described. Total murine IgA was measured using the Mouse IgA ELISA kit per manufacturer's protocol (eBioscience).

2.4. Cytokine secretion assay

Isolation and culture of lamina propria mononuclear cells (LPMC) and mesenteric lymph node cells (MLN) were carried out as previously reported (Shih et al., 2011) MLN and LPMC were plated at 2.5×10^5 cells/well in 96 well plates in RPMI 1640 medium (cellgro) with 10% fetal calf serum, 100 U/ml penicillin, 100 mg/ml gentamycin, 2 mM L-glutamine and stimulated with 2 μL/ml LK Activation cocktail for 4 h. The expression of TNF-α, IL-6 and IL-1β in cell supernatants were assayed by ELISA according to manufacturer's instructions (Mouse TNF-α ELISA Ready-Set-Go, eBioscience, 88–7324-77; Mouse IL-1β ELISA Ready-SET-Go, eBioscience, 88–7013-77; Mouse IL-6 ELISA Ready-SET-Go, eBioscience, 88–7064-77).

2.5. Western blot

BMDCs were derived from Atg16l1$^{f/f}$ and Atg16l1ΔDC mice (Shouval et al., 2014). BMDCs were cultured in 20 ng/ml mouse GM-CSF (PeproTech, 315-03) for 12 days and were stimulated with 100 ng/ml mouse LPS-EK (InvivoGen, tlrl-eklps) overnight before different assays. Cells were plated on 6-well plates at 1500,000 cells/well overnight and were infected with *S. typhimurium* at a multiplicity of infection (MOI) of 1:20 for 60 min. After stimulation, cells were lysed in LDS sample buffer (Novex, NP0007), boiled, and added onto SDS-polyacrylamide gels (Invitrogen, NP0341BOX). Proteins were transferred to polyvinylidenedifluoride membranes (Fisher-Scientific, 07-200-165), blocked for 60 min with 1% BSA, and stained overnight with the indicated primary antibody (LC3, Cell Signaling, 3868; P62, Sigma-Aldrich, P0067; b-actin, Cell Signaling, 8457; Phospho-p40phox (Thr154) Antibody, Cell Signaling, 4311; Atg16l1 D6D5, Cell Signaling) at 4 °C. Blots were washed and stained with HRP-conjugated secondary antibody (Goat ant-rabbit

IgG-HRP, Santa-Cruz, sc-2004), and binding was detected by chemiluminescence (Thermo Scientific, 34080).

2.6. Uptake and ROS assays

Cells were plated on 24-well plates at 500,000 cells/well overnight and infected with *S. typhimurium* at a MOI of 1:20 for 15 min, 30 min and 60 min. After stimulation, cells were washed and fixed in 2% paraformaldehyde, permed for 20 min with perm buffer, and stained for 45 min with the indicated primary Abs (abcam, ab8274) at room temperature. Cells were washed and stained with goat anti-mouse IgG H&L secondary antibody (abcam, ab96873), and fluorescence were detected by flow cytometry. ROS production was detected by luminol-ECL (sigma, A8511-5G) as previously described (Ma et al., 2014).

2.7. Gentamycin protection assays

Intracellular *S. typhimurium* killing was assessed by gentamycin protection assay. Cells were infected with *S. typhimurium* at a MOI of 1:20 for 30 min, and further incubated in gentamycin-supplemented DMEM (50 μg/ml) or gentamycin-supplemented EBSS for 1 h or 4hs. BMDCs were lysed in 1% Triton/PBS for 10 min on ice and serial dilutions plated on LB agar and grown overnight at 37 °C. Colonies recovered were counted and CFU per well were calculated.

2.8. Transmission electron microscopy (TEM)

Cells were harvested, pelleted and fixed in 2.5% glutaraldehyde and 2% paraformaldehyde in PBS. And then the samples were processed by the UCLA EM-Core.

2.9. Antigen presentation assay

As previously reported (Tobar et al., 2006). Isolated $CD4^+$ T cells were isolated using the EasySep™ Mouse $CD4^+$ T Cell Isolation kit (Stem Cell) from spleen from OT-II/RAG2 mice and stained with Cell Trace CSFE (Thermo Fisher Scientific) according to manufacturer's recommendations. CFSE stained cells were co-cultured (1BMM to 4 CD4+ T cells) with either $Atg16l1^{f/f}$ or Atg16l1 deficient BMDCs that were exposed to whole OVA or OVA peptide 323–339 for 6 h. Cells from 72 h co-cultures were collected and stained with CD4 GK1.5 (Biolegend) and Live-Dead stain (Fisher Scientific). After gating on live $CD4^+$ T cells, CFSE staining was analyzed by flow cytometry to determine the $CD4^+$ T cell proliferation. Cells were also stained with MCHII (Biolegend), CD86 (Biolegend) and D80 (Biolegend) to detect the activity of those cells. The expression of TNF-α and IL-1β in cell supernatants were assayed by ELISA according to manufacturer's instructions (Mouse TNF-α ELISA Ready-Set-Go, eBioscience, 88–7324-77; Mouse IL-1β ELISA Ready-SET-Go, eBioscience, 88–7013-77).

2.10. Statistical analysis

Data are presented as the mean ± standard deviation (SD). Comparison between two groups was performed by a two-tailed Fisher's Exact Test for categorical variables and Student's *t*-test for continuous variables. Parametric and non-parametric tests were used depending on the fulfillment of the test assumptions. Comparison between three groups was done using

ANOVA, followed by pair wise post-hoc analysis with Turkey's HSD and Behrens-fisher-Test correction for the multiple comparisons. $P < 0.05$ was considered significant.

3. Results

3.1. Atg16l1 deficiency in CD11c$^+$ DCs exacerbated DSS-induced murine colitis

Atg16l1 deficiency is lethal for mice (Tobar et al., 2006; Kuma et al., 2004). Atg16l1$^{f/f}$ mice and Atg16l1ΔDC mice using CD11c-Cre were generated so that the role of Atg16l1 in gut mucosal homeostasis could be assessed *in vivo* colitis models (Fig. 1A). Atg16l1 deficiency in BMDCs was confirmed by the lack of Atg16l1 mRNA and protein (Fig. 1B, C). BMDCs with Atg16l1 deficiency also exhibited functional autophagy deficiency as shown by the impaired conversion of LC3-I to LC3-II conversion (Fig. 1C).

Two acute models and one chronic model of murine colitis were performed to clarify the specific effects of Atg16l1 on murine colitis. For the *S. typhimurium* infection model, after pilot time-course experiments, we chose 5 days for our analyses, which is different from published reports (Murthy et al., 2014). There was no significant different in DAI and histologic examination of colon between Atg16l1$^{f/f}$ mice and Atg16l1ΔDC mice in salmonella infection model. In DSS-induced colitis models, significant increased DAI were observed in Atg16l1ΔDC mice as compared to control Atg16l1$^{f/f}$ mice (Fig. 1D). Histological examination of the colon revealed worsened inflammation characterized by increased cellular infiltrate, mucin depletion, crypt abscess, and architectural changes in Atg16l1ΔDC mice as compared to Atg16l1$^{f/f}$ mice only in DSS-induced colitis models, suggesting that these mice are more susceptible to DSS-induced inflammation after damage of epithelium barrier (Fig. 1E).

3.2. Increased IgA-coated bacteria in the stool of Atg16l1ΔDC mice

IgA is the predominant antibody isotype in the gut mucosa that coats pathogens and provides protection against infection through neutralization and exclusion (Palm et al., 2014). IgA coating has been shown to identify IBD-driving microbes in mice and humans (Pabst, 2012). To assess whether IgA coating of fecal bacteria plays a role in exacerbation of murine colitis observed with Atg16l1 deficiency in CD11c$^+$ DCs, we examined IgA staining in stool collected from Atg16l1$^{f/f}$ and Atg16l1ΔDC mice. Flow cytometry showed that Atg16l1ΔDC mice had increased IgA-coating of bacteria compared to control Atg16l1$^{f/f}$ mice (Fig. 2). Total IgA in the stools was quantitated by IgA ELISA to determine whether increased IgA coating of fecal bacteria was due to increased IgA secretion into the intestinal lumen. Total stool IgA was increased in the *S. typhimurium* infection model but not in acute or chronic DSS model (Fig. 2B). Together, these data suggested that there was an increase in colitogenic IgA-coated microbiota in Atg16l1ΔDC mice that may contribute to exacerbated colitis with Atg16l1 deficiency in CD11c$^+$ DCs.

3.3. Atg16l1 deficiency increased proinflammatory cytokines

Autophagy inhibits inflammation through the down-regulation of inflammasome formation and pro-IL-1β cleavage to its active form (Mizushima et al., 2003). A previous paper has shown that IL-1β production is enhanced upon autophagy deficiency, leading to gut

inflammation in mice with reduced autophagy levels (Atg16l1 hypomorphic mice) (Harris et al., 2011). In our study, analysis of inflammatory cytokines of tumor necrosis factor-α (TNF-α), IL-6 and IL-1β from MLN and LPMC was performed by ELISA in all the models to detect their ability in producing proinflammatory cytokines. Significantly increased IL-1β and TNF-α, but not IL-6 was observed in Atg16l1ΔDC mice as compared to Atg16l1$^{f/f}$ mice in both MLN and LPMC only in DSS-induced colitis models (Fig. 3; data for the *S. typhimirium* infection model were showed in the supplementary materials). Consistently, our data suggest that loss of autophagy in CD11c^{+} DCs is associated with exaggerated proinflammatory cytokine responses, which may be one of the mechanisms of exacerbating colitis in Atg16l1 deficiency mice.

3.4. Functional assay of BMDCs

To further establish the important role of autophagy in BMDCs, the functional assay was assessed in our experiment. These cells were stimulated under various autophagy conditions including starvation and *S. typhimurium* infection. Various assays of western blot, uptake of *S. typhimurium*, ROS production, intracellular killing, antigen presentation, and TEM were performed to illuminate the functional role of Atg16l1 *in vitro*.

3.4.1. Atg16l1 deficient BMDCs show autophagy deficient by western blot— Atg16l1 is a key component of the autophagy machinery and functions through its interaction with an ATG5-ATG12 conjugate to direct the site of autophagosome formation (VanDussen et al., 2014; Lupfer et al., 2013; Fujita et al., 2008). Recruitment of Atg16l1:ATG5-ATG12 promotes the localized conversion of LC3 to a phosphotidyl-ethanolamine-conjugated form, LC3-II, and thus induces the formation of autophagosome (Lupfer et al., 2013). As predicted, we consistently observed that Atg16l1 deficient BMDCs led to reduction in LC3 II production when the autophagy of BMDCs was induced by both starvation and *S. typhimurium*. Autophagy was functionally impaired in Atg16l1 deficient BMDCs as compared to Atg16l1$^{f/f}$ BMDCs (Fig. 4A).

3.4.2. Uptake of *S. typhimurium*, ROS production and gentamycin protection assay—In our experiment, there was no difference in uptake of *S. typhimurium* between Atg16l1$^{f/f}$ BMDCs and autophagy gene Atg16l1 deficient BMDCs at 15 min, 30 min, and 60 min post infection (Fig. 4B). However, Atg16l1 deficient BMDCs have increased ROS production when stimulated with *S. typhimurium* (Fig. 4C). Similar results were obtained when the cells were stimulated with zymosan (Fig. 4C), a ligand found on the surface of fungi. Despite the increase of ROS production in autophagy deficient BMDCs, we found that there is actually an increase in intracellular *S. typhimurium* survival in autophagy deficient BMDCs (Fig. 4D).

Because one of the cellular machinery for ROS production is NADPH oxidase complex, and neutrophil cytosol factor 40 or p40Phox is a cytosolic regulatory component of the superoxide-producing phagocyte NADPH-oxidase, we measured the phosphorylation of the cytosolic p40 subunit of the NADPH oxidase by western blot. Higher p40Phox is correlated with increased ROS production. Consistently, there was increased expression of p40Phox in the Atg16l1 deficient BMDCs (Fig. 4A).

In addition, mitochondrial number with Atg16l1 deficiency was assessed since mitochondria provide another significant cellular source of ROS. Consistent with the role of autophagy in removing dysfunctional mitochondria, there were increased mitochondria in the DCs with Atg16l1 deficiency as compared to Atg16l1$^{f/f}$ BMDCs (Fig. 5D). Together, Atg16l1 deficiency led to increased oxidative stress and ROS both at baseline and with *S. typhimurium* infection concomitant with increased activation of NADPH oxidase and mitochondria number.

3.4.3. Transmission electron microscope (TEM) for autophagosomes and phagosomes—To make sure there is indeed lack of double membrane autophagy vesicles, and a shifting of intracellular *S. typhimurium* to phagosomes in the Atg16l1 deficient BMDCs, TEM was performed in our experiment. At baseline, there are very few autophagy and phagocytosis vesicles in BMDCs. Infection with *S. typhimurium* resulted in an increase in the number of phagosomes and autophagosomes in Atg16l1$^{f/f}$ BMDCs but only of phagosomes in the Atg16l1 deficient BMDCs. Under starvation condition, there was a shifting of vesicles to the autophagy pathway in Atg16l1$^{f/f}$ BMDCs but not in the Atg16l1 deficient BMDCs (Fig. 5A). This may reflect that autophagy vesicles are formed prior to deletion of the Atg16l1 gene. By TEM, we observed reduced numbers of *S. typhimurium* in double membrane vacuoles in Atg16l1 deficient BMDCs (Fig. 5B) and increased numbers of *S. typhimurium* in single membrane vacuoles (Fig. 5C), indicating that the risk variant is associated with reduced autophagy. These data suggest that there is indeed lack of double membrane autophagy vesicles and shifting of intracellular *S. typhimurium* to phagosomes in Atg16l1 deficient BMDCs.

3.5. Atg16l1 is required for processing of antigens for MHC II

Constitutive activation of autophagy in MHC II-positive cells including DCs has previously been demonstrated (Fujita et al., 2009). A marked reduction in MHC II antigen presentation in autophagy-inhibited DCs was found. To further evaluate this notion, we pulsed Atg16l1$^{f/f}$ BMDCs and Atg16l1 deficient DCs with $OVA_{323–339}$ that do not need further intracellular processing but still require uptake of antigen and loading of antigen to MHC-II. Using $OVA_{323–339}$, similar stimulation of $CD4^+$ T cells proliferation was observed in Atg16l1$^{f/f}$ BMDCs compared to Atg16l1 deficient BMDCs (Fig. 6A). Reduced proliferation of $CD4^+$ T cells was observed in Atg16l1 deficient BMDCs compared to Atg16l1$^{f/f}$ BMDCs when using OVA-full length protein that needs further intracellular processing. To rule out the difference of the cell activation, we checked the activation markers. The deletion of ATG16L1 did not affect the expressions of MHC-II, CD80 and CD86 (Fig. 6C) in BMDCs as well as the TNF-α and IL-1β production (Fig. 6D). Together, these data indicated that the impaired presentation of antigen by DCs to $CD4^+$ T cells is due to altered processing of antigen and not due to uptake of antigen into cells or loading of antigen to MHC-II protein or the difference of cell activation.

4. Discussion

Previous studies showed that ATG16L1 function in epithelial cells, but not in DC, was required for intestinal homeostasis (Conway et al., 2013). In our current study, two acute and

one chronic models of murine colitis were performed to clarify specific effects of Atg16l1 on $CD11c^+$ DCs. We showed that compared to $Atg16l1^{f/f}$ mice, the increased histological inflammation was found in Atg16l1ΔDC mice only in DSS-induced colitis, suggesting that autophagy deficiency in $CD11c^+$ DCs exacerbated inflammation only after damage of epithelial cells. Accumulating studies have highlighted the fact that IL-1β production is enhanced upon autophagy deficiency leading to gut inflammation in mice with reduced autophagy levels (Atg16l1 hypomorphic mice) (Sorbara et al., 2013). Saitoh et al. demonstrated that LPS induced IL-1β secretion in embryonic liver macrophages from $Atg16L^{-/-}$ mice in a TIR-domain-containing adapter-inducing interferon-â (TRIF)-dependent manner, suggesting the role of autophagy in secretion of IL-1β (Saitoh et al., 2008). Inhibition of autophagy stimulated the production of IL-1β by bone marrow-derived macrophages in an NLRP3-dependent manner (Schmid et al., 2007). In line with the literary reported, our current study showed that in addition to TNF-α, increased pro-inflammatory of IL-1β in Atg16l1ΔDC mice, resulting in intestinal inflammation. Therefore, impaired ATG16L1 function led to increased pro-inflammatory cytokines *in vivo*, which is one of the novel mechanisms of IBD.

Several independent GWAS have linked defects in autophagy, a crucial element in the innate immune response to intracellular pathogens, to the pathogenesis of CD (Cho and Brant, 2011). Autophagy is a potent mechanism for restraining adherent-invasive Escherichia coli (AIEC) intracellular replication within epithelial cells (Carvalho et al., 2009). Another recent study shows that induction of autophagy allows macrophages to restrain the number of intracellular AIEC bacteria (Lapaquette et al., 2012). Coincident with the previous studies, our study demonstrated that Atg16l1 deficiency leaded to decrease in intracellular *S. typhimurium* killing, suggesting that the impaired bacteria clearance with ATG16L1 deficiency could lead to increased number of colitogenic bacteria that contributed to murine colitis. Recently, IgA-coated bacteria were implicated as IBD-promoting microbes (Pabst, 2012). Consistently, we observed that increased amounts of IgA-coated bacteria were found in mice with Atg16l1 deficiency, which was further increased in the context of intestinal inflammation.

ATG16L1 is a key component of the autophagy machinery. ATG16L1 functions in autophagy through its interaction with an ATG5-ATG12 conjugate to direct the site of autophagosome formation. Recruitment of ATG16L1:ATG5-ATG12 promotes the localized conversion of LC3 to a phosphotidyl-ethanolamine-conjugated form, LC3-II, and thus drives autophagosome formation (Sorbara et al., 2013). As expected, ATG16L1 deficiency led to impaired conversion of endogenous LC3-I to LC3-II after starvation or *S. typhimurium* treatment and defective targeting of intracellular *S. typhimurium* to autophagosomes.

DCs are key elements for the generation of an efficient adaptive immune response against bacterial pathogens. They have the unique ability to initiate adaptive immunity by activating naive T cells (Tobar et al., 2006). We further demonstrated that ATG16L1 deficiency resulted in defective processing of antigens onto MHC-II to activate naive T cells. Insufficient activation of the adaptive immune response with ATG16L1 deficiency could be sufficient to explain ineffective elimination of pathogenic bacteria and the activation of intestinal inflammation in DSS-induced colitis model.

Saitoh et al. (Saitoh et al., 2008) found that Atg16l1 deficient macrophages generated higher levels of ROS in response to LPS compared with WT cells, suggesting that autophagy is an important regulator of intracellular ROS. In line with the previous data, our studies demonstrate that autophagy deficient $CD11c^+$ DCs show exacerbated production of ROS, which may contribute to intestinal inflammation. The increased ROS production with ATG16L1 deficiency was in part due to increased NADPH oxidase complex and altered mitochondria number.

5. Conclusion

In conclusion, our study reveals that specific disruption of autophagy in $CD11c^+$ DCs exacerbates DSS-induced colitis by exacerbating IL-1β and TNF-α production. Atg16l1 deficiency leads to increase in p40Phox and ROS production, decrease in intracellular *S. typhimurium* killing, shift of *S. typhimurium* to phagocytosis vesicles. These results identify $CD11c^+$ DCs autophagy as a novel protective pathway during colitis, which may be related to down-regulation of IL-1β and TNF-α-driven inflammation, IgA^+ bacteria, antigen processing and appropriate ROS production.

Acknowledgments

The authors gratefully acknowledge the financial support from Cedars-Sinai Inflammatory Bowel and Immunobiology Research Institute. We thank all members of Cedars-Sinai Inflammatory Bowel and Immunobiology Research Institute for their contributions to this work. Papers using specimens, data, or analysis provided by the MIRIAD Biobank. MIRIAD is currently Supported by F Widjaja Foundation Inflammatory Bowel and Immunobiology Research Institute, NIH grant P01DK046763, The European Union Grant 305479, NIDDK Grant DK062413, U54 DK102557, and The Leona M and Harry B Helmsley Charitable Trust.

References

Banchereau J, Briere F, Caux C, et al. Immunobiology of dendritic cells. Annu. Rev. Immunol. 2000; 18:767–811. [PubMed: 10837075]

Barrett R, Zhang X, Koon HW, et al. Constitutive TL1A expression under colitogenic conditions modulates the severity and location of gut mucosal inflammation and induces fibrostenosis. Am. J. Pathol. 2012; 180:636–649. [PubMed: 22138299]

Barthel, Manja, Hapfelmeier, Siegfried, Quintanilla-Martínez, L., et al. Pretreatment of mice with streptomycin provides a Salmonella enterica Serovar Typhimurium Colitis model that allows analysis of both pathogen and host. Infect. Immun. 2003:2839–2858. [PubMed: 12704158]

Carvalho FA, Barnich N, Sivignon A, et al. Crohn's disease adherent-invasive Escherichia coli colonize and induce strong gut inflammation in transgenic mice expressing human CEACAM. J. Exp. Med. 2009; 206:2179–2189. [PubMed: 19737864]

Castillo EF, Dekonenko A, Arko-Mensah J, et al. Autophagy protects against active tuberculosis by suppressing bacterial burden and inflammation. Proc. Natl. Acad. Sci. U. S. A. 2012; 109:E3168–E3176. [PubMed: 23093667]

Cho JH, Brant SR. Recent insights into the genetics of inflammatory bowel disease. Gastroenterology. 2011; 140:1704–1712. [PubMed: 21530736]

Congcong H, Daniel JK. Regulation mechanisms and signaling pathways of autophagy. Annu. Rev. Genet. 2009; 43:67–93. [PubMed: 19653858]

Conway KL, Kuballa P, Song JH, et al. Atg16l1 is required for autophagy in intestinal epithelial cells and protection of mice from Salmonella infection. Gastroenterology. 2013; 145:1347–1357. [PubMed: 23973919]

Cooney R, Baker J, Brain O, et al. NOD2 stimulation induces autophagy in dendritic cells influencing bacterial handling and antigen presentation. Nat. Med. 2009; 16:90–97. [PubMed: 19966812]

Fujita N, Matsunaga K, Noda T, et al. Molecular mechanism of autophagosome formation in mammalian cells. Tanpakushitsu Kakusan Koso. 2008; 53:2106–2110. [PubMed: 21038593]

Fujita N, Noda T, Yoshimori T. Atg4 B (C74A) hampers autophagosome closure: a useful protein for inhibiting autophagy. Autophagy. 2009; 5:88–89. [PubMed: 19104152]

Györgyi M, Zsolt T, Ferenc S. Interplay of autophagy and innate immunity in Crohn's disease: a key immunobiologic feature. World J. Gastroenterol. 2013; 19:4447–4454. [PubMed: 23901219]

Harris J, Hartman M, Roche C, et al. Autophagy controls IL-1 beta secretion by targeting pro-IL-1 beta for degradation. J. Biol. Chem. 2011; 286:9587–9597. [PubMed: 21228274]

Messer, Jeannette S., Murphy, Stephen F., Logsdon, Mark F., et al. The Crohn's disease: associated ATG16L1 variant and Salmonella invasion. BMJ Open. 2013; 3:e002790.

Kuballa P, Huett A, Rioux JD, et al. Impaired autophagy of an intracellular pathogen induced by a Crohn's disease associated ATG16L1 variant. PLoS One. 2008; 3:e3391. [PubMed: 18852889]

Kuma A, Hatano M, Matsui M, et al. The role of autophagy during the early neonatal starvation period. Nature. 2004; 432:1032–1036. [PubMed: 15525940]

Lapaquette P, Bringer MA, Darfeuille-Michaud A. Defects in autophagy favour adherent-invasive Escherichia coli persistence within macrophages leading to increased pro-inflammatory response. Cell. Microbiol. 2012; 14:791–807. [PubMed: 22309232]

Lassen G, Kuballa P, Conway KL, et al. Atg16L1 T300A variant decreases selective autophagy resulting in altered cytokine signaling and decreased antibacterial defense. Proc. Natl. Acad. Sci. 2014; 111:7741–7746. [PubMed: 24821797]

Lee HK, Mattei LM, Steinberg BE, et al. In vivo requirement for Atg5 in antigen presentation by dendritic cells. Immunity. 2010; 32:227–239. [PubMed: 20171125]

Lupfer C, Thomas PG, Anand PK, et al. Receptor interacting protein kinase 2-mediated mitophagy regulates inflammasome activation during virus infection. Nat. Immunol. 2013; 14:480–488. [PubMed: 23525089]

Ma J, Becker C, Reyes C, et al. Cutting edge: FYCO1 recruitment to dectin-1 phagosomes is accelerated by light chain 3 protein and regulates phagosome maturation and reactive oxygen production. J. Immunol. 2014; 192:1356–1360. [PubMed: 24442442]

Mizushima N, Kuma A, Kobayashi Y, et al. Mouse Apg16L, a novel WD-repeat protein, targets to the autophagic isolation membrane with the Apg12-Apg5 conjugate. J. Cell Sci. 2003; 116:1679–1688. [PubMed: 12665549]

Murthy A, Li Y, Peng I, et al. A Crohn's disease variant in Atg16l1 enhances its degradation by caspase 3. Nature. 2014; 506:456–462. [PubMed: 24553140]

Pabst O. New concepts in the generation and functions of IgA. Nat. Rev. Immunol. 2012; 12:821–832. [PubMed: 23103985]

Palm N, de Zoete MR, Cullen TW, et al. Immunoglobulin A coating identifies colitogenic bacteria in inflammatory bowel disease. Cell. 2014; 158:1000–1010. [PubMed: 25171403]

Reed M, Morris SH, Jang S, et al. Autophagy-inducing protein beclin-1 in dendritic cells regulates $CD4^+$ T cell responses and disease severity during respiratory syncytial virus infection. J. Immunol. 2013; 191:2526–2537. [PubMed: 23894198]

Reise SC. Dendritic cells in a mature age. Nat. Rev. Immunol. 2006; 6:476–483. [PubMed: 16691244]

Rescigno M, Di Sabatino A. Dendritic cells in intestinal homeostasis and disease. J. Clin. Invest. 2009; 119:2441–2450. [PubMed: 19729841]

Saitoh T, Fujita N, Jang MH, et al. Loss of the autophagy protein Atg16l1 enhances endotoxin-induced IL-1beta production. Nature. 2008; 456:264–268. [PubMed: 18849965]

Salio M, Puleston DJ, Mathan TS, et al. Essential role for autophagy during invariant NKT cell development. PNAS. 2014; 111:E5678–E5687. [PubMed: 25512546]

Schmid D, Pypaert M, Münz C. Antigen-loading compartments for major histocompatibility complex class II molecules continuously receive input from autophagosomes. Immunity. 2007; 26:79–92. [PubMed: 17182262]

Shih DQ, Barrett R, Zhang X, et al. Constitutive TL1A (TNFSF15) expression on lymphoid or myeloid cells leads to mild intestinal inflammation and fibrosis. PLoS One. 2011; 6:e16090. [PubMed: 21264313]

Shouval DS, Biswas A, Goettel JA, et al. Interleukin-10 receptor signaling in innate immune cells regulates mucosal immune tolerance and anti inflammatory macrophage function. Immunity. 2014; 40:706–719. [PubMed: 24792912]

Sorbara MT, Ellison LK, Ramjeet M, et al. The protein Atg16l1 suppresses inflammatory cytokines induced by the intracellular sensors Nod1 and Nod2 in an autophagy-independent manner. Immunity. 2013; 39:858–873. [PubMed: 24238340]

Tobar JA, Carreño L, Bueno SM, et al. Virulent Salmonella enterica serovar typhimurium evades adaptive immunity by preventing dendritic cells from activating T cells. Infect. Immun. 2006; 11:6438–6448.

VanDussen KL, Liu TC, Li D, et al. Genetic variants synthesize to produce paneth cell phenotypes that define subtypes of Crohn's disease. Gastroenterology. 2014; 146:200–209. [PubMed: 24076061]

Zhang H, Zheng L, McGovern DP, et al. Myeloid ATG16L1 facilitates host-bacteria interactions in maintaining intestinal homeostasis. J. Immunol. 2017; 198:2133–2146. [PubMed: 28130498]

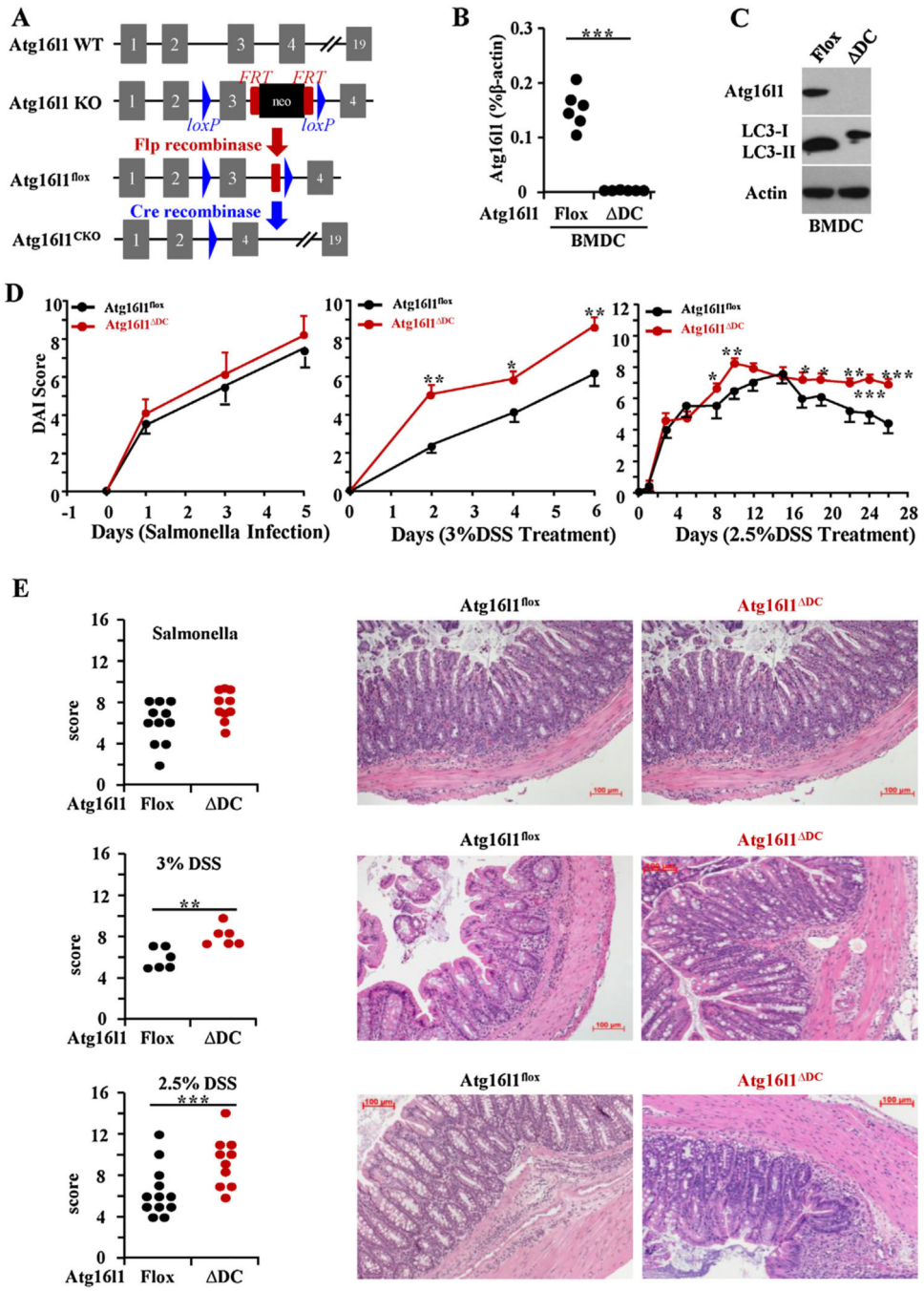

Fig. 1.

Loss of Atg16l1 in dendritic cells (DCs) exacerbated DSS-induced murine models of colitis. (A) Schematic of Atg16l1 gene targeting. (B) RT-PCR of Atg16l1 mRNA in mouse bone marrow-derived dendritic cells (BMDC). Each filled circle represents an independent experiment and data are expressed as percent of β-actin expression (n = 6). (C) Representative western blot of Atg16l1, LC3 and β-actin was shown (n = 6). (D) Disease activity index of *S. typhimurium* infection model (n = 12–14 per group), acute DSS-induce colitis model (n = 6 per group), and chronic DSS-induced colitis model (n = 10-19 per

group) were quantitated and are shown. Scale bar represents 100 μm. (E) Representative H&E stained mid-colon sections from 6 to 8 weeks old mice at 100× magnification is shown and data from multiple mice are quantitated (n = 10–12 per group). (* $P < 0.05$, ** $P < 0.01$, *** $P < 0.001$).

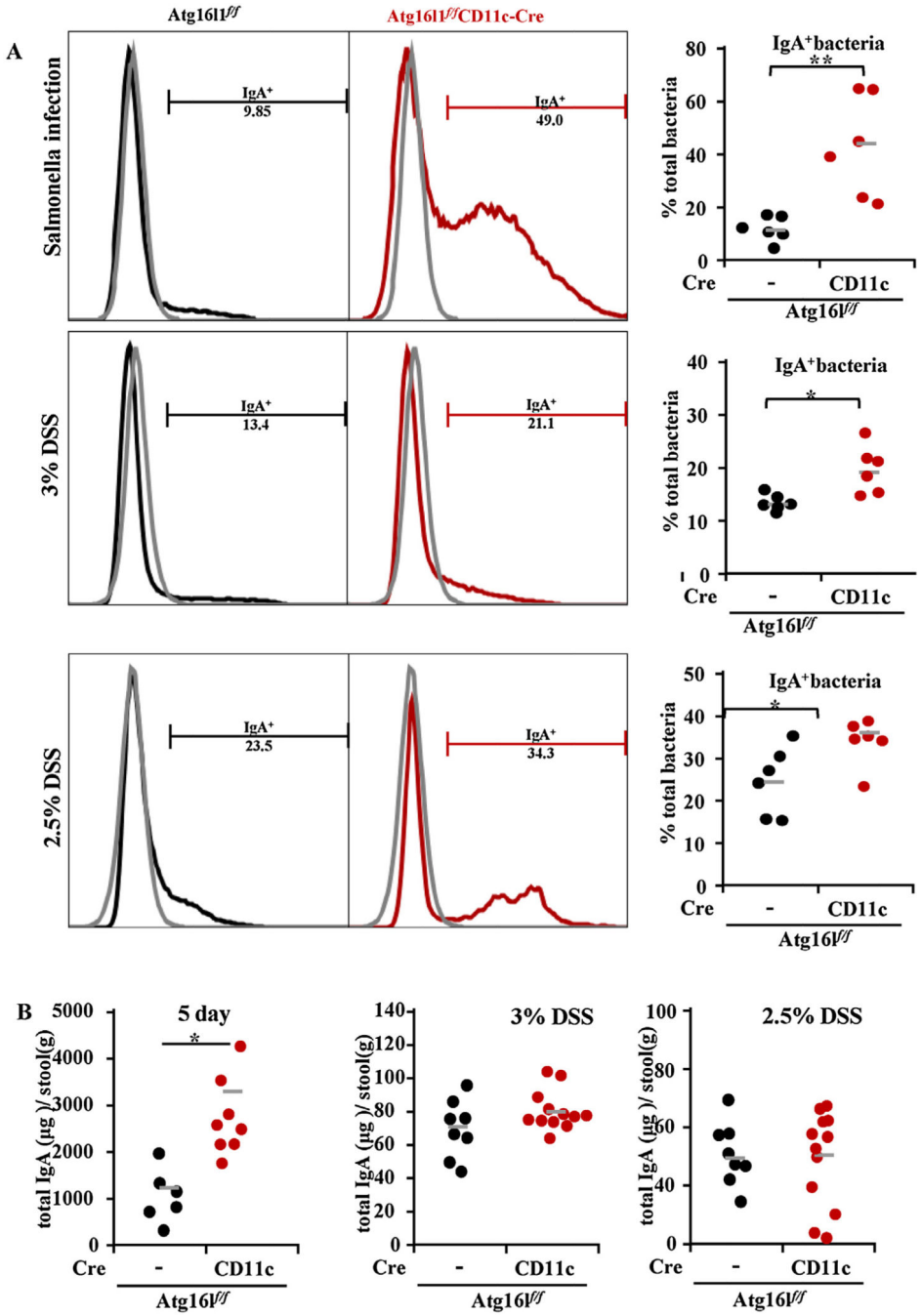

Fig. 2.

Increased IgA-coated bacteria in the stool of mice with Atg16l1 deficiency in DCs. (A) Representative flow cytometry plots of fecal bacteria stained with anti-IgA antibody from mice undergoing the 3 colitis models were shown and quantitated (The gray plot indicates unstained sample; the black plot indicates samples form Atg16l1$^{f/f}$ mice; the red plot indicates samples from Atg16L1$^{f/f}$ *CD11c-Cre* mice). (B) Total IgA in the stools was quantitated by IgA ELISA and represented as microgram (μg) of IgA per gram (g) of stool).

Data were expressed as mean ± SEM. (*$P < 0.05$). (For interpretation of the references to colour in this figure legend, the reader is referred to the web version of this article.).

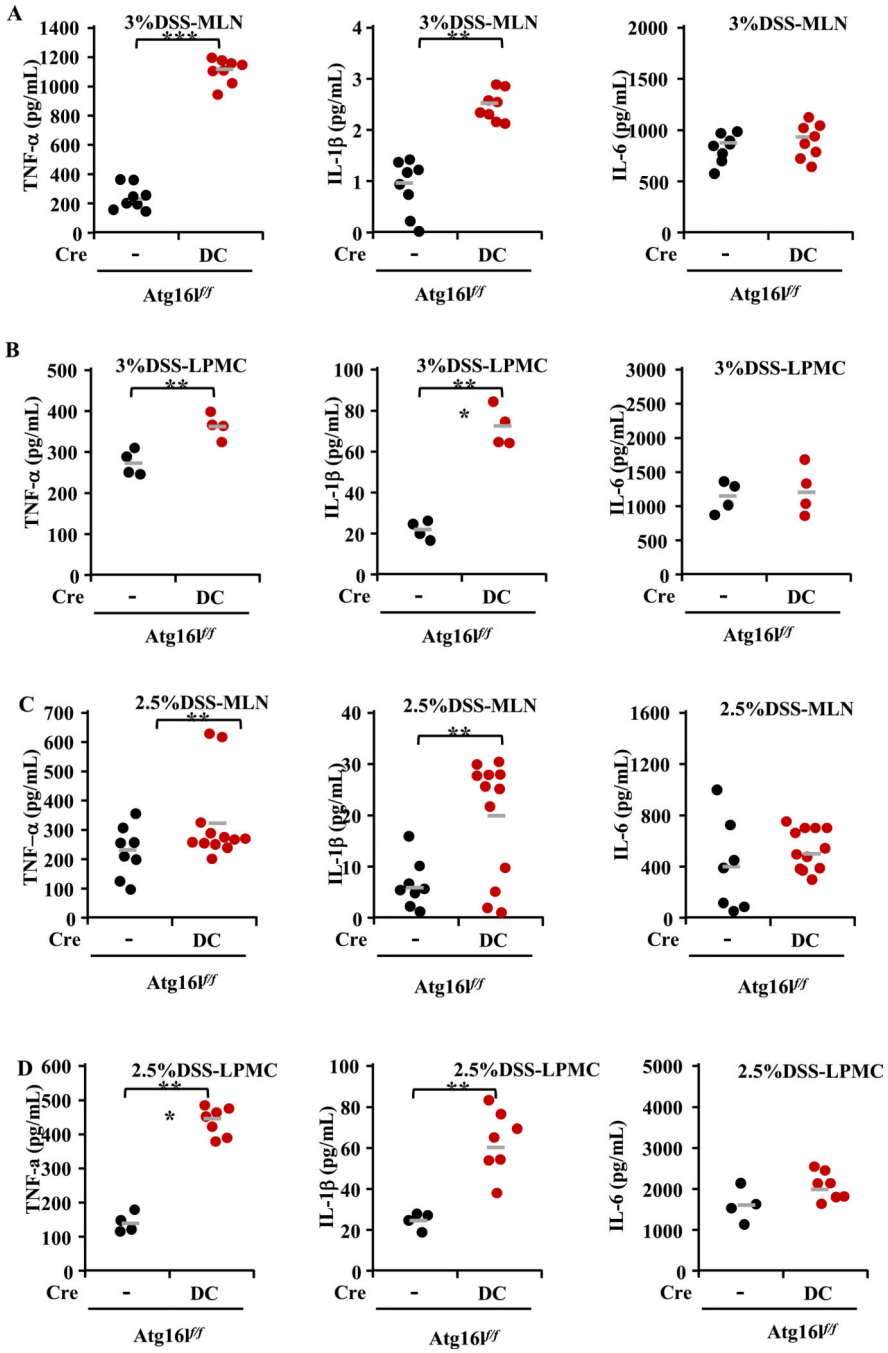

Fig. 3.

Increased expressions of IL-1β, TNF-α, not IL-6 detected by ELISA with Atg16l1 deficiency in DCs. (A) The expressions of TNF-α, IL-6 and IL-1β in MLN in 3% DSS model at day 7. (B) The expressions of TNF-α, IL-6 and IL-1β in LPMC in 3% DSS model at day 7. (C) The expressions of TNF-α, IL-6 and IL-1β in MLN in 2.5% DSS model at day 29. (D) The expressions of TNF-α, IL-6 and IL-1β in LPMC in 2.5% DSS model at day 29. Higher cytokines production of TNF-α and IL-1β was observed in Atg16L1$^{f/f}$ *CD11c-Cre*

mice as compared to control Atg16l1^{flf} mice in MLN and LPMC in DSS-induced colitis models (*$P < 0.05$, **$P < 0.01$, ***$P < 0.001$).

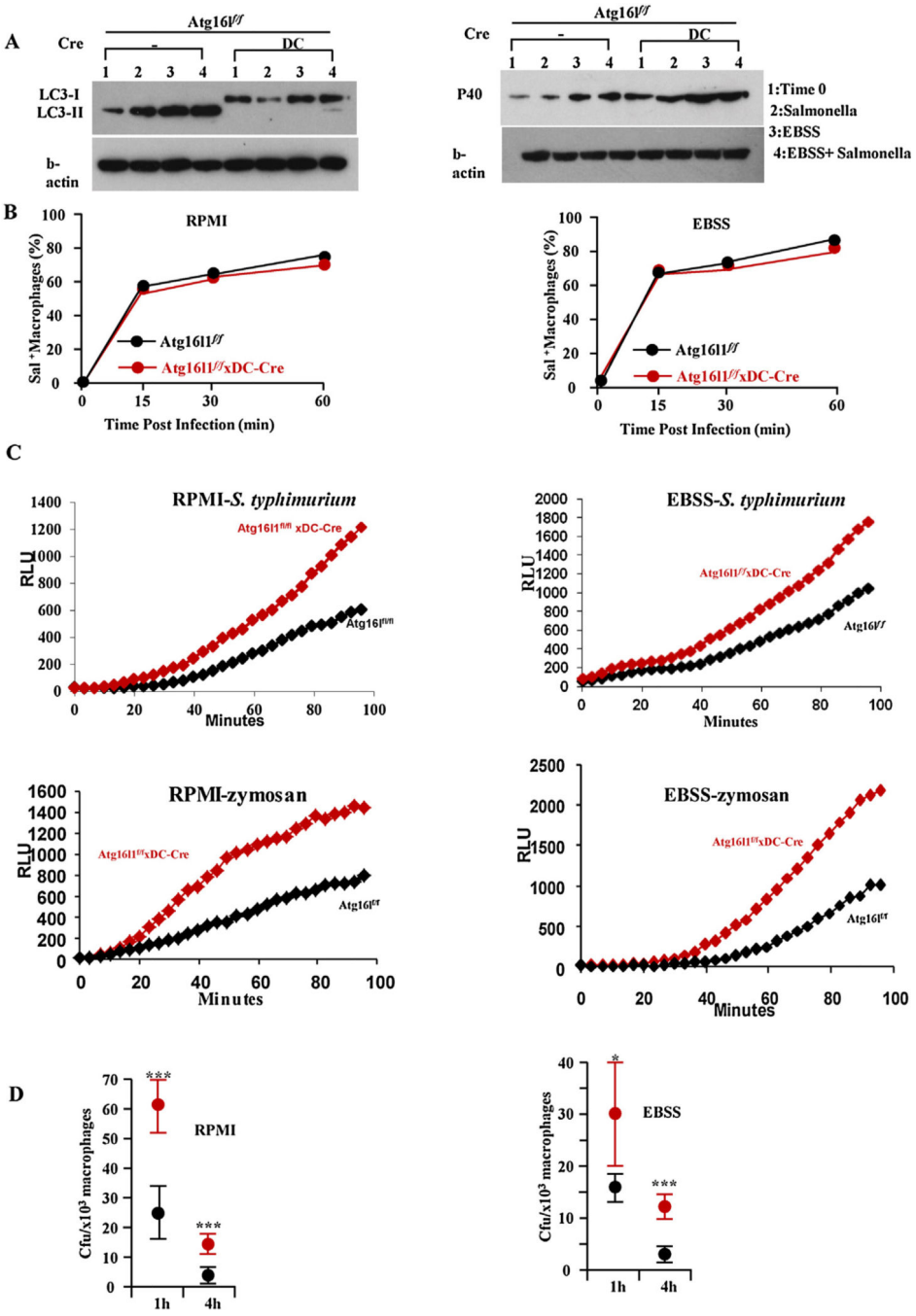

Fig. 4.

Atg16l1 deficient BMDCs have increased ROS production but reduced killing of *S. typhimurium*. (A) Western blots of LC3, Phospho-p40phox and β-actin in Atg16l1$^{f/f}$ and Atg16l1ΔDC BMDCs. (B) The uptake of *S. typhimurium* in BMDCs under rich (RPMI) and starvation (EBSS) conditions. (C) Relative ROS production as measured by luminol-dependent chemiluminescence was determined over 60 min for BMDCs from Atg16l1$^{f/f}$ and Atg16l1ΔDC mice treated with *S. typhimurium* or zymosan. (D) Higher intracellular *S. typhimurium* recovered in Atg16l1 deficient BMDCs (red dot) compared to Atg16l1$^{f/f}$

BMDCs (black dot). (n = 8, *$P < 0.05$, ***$P < 0.001$). (For interpretation of the references to colour in this figure legend, the reader is referred to the web version of this article.)

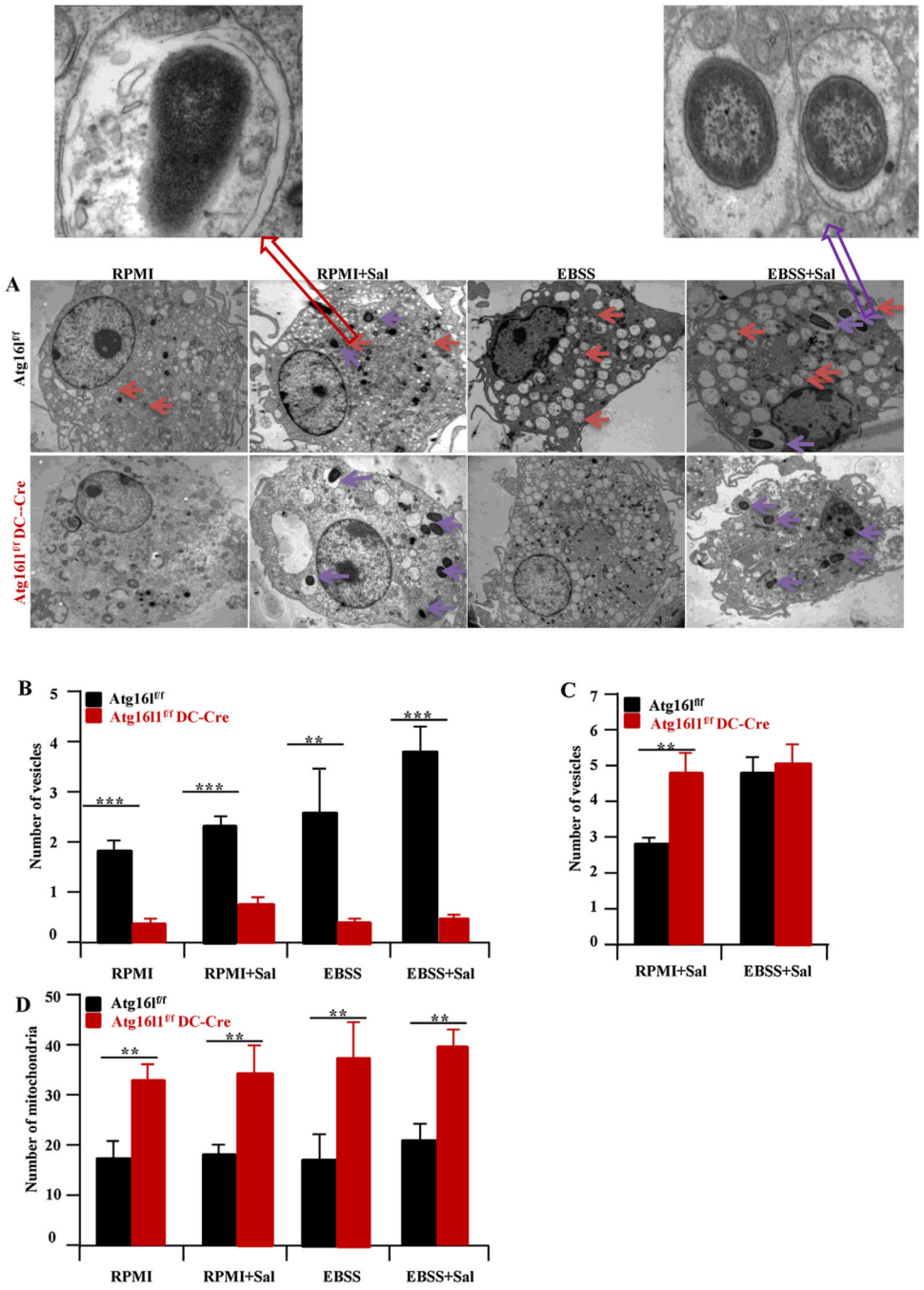

Fig. 5.

Transmission electron microscopy of BMDCs. (A) Representative photograph of BMDCs from Atg16l1$^{f/f}$ and Atg16l1ΔDC mice are shown (top panels). Single membrane vesicles (denotes phagocytosis vesicles) (B), double membrane vesicles (denotes autophagy vesicles) (C) and mitochondria (D) are quantitated and shown. There is a shift from double to single membrane vesicles in the Atg16l1 deficient as compared to Atg16l1$^{f/f}$ BMDC. Red arrow denotes double membrane vesicle. Purple arrow denotes single membrane vesicle. The number of mitochondria in the Atg16l1 deficient BMDCs is higher compared to Atg16l1$^{f/f}$

BMDCs. (n = 8, $^{**}P < 0.01$, $^{***}P < 0.001$) autophagy and phagocytosis vesicles. (For interpretation of the references to colour in this figure legend, the reader is referred to the web version of this article.)

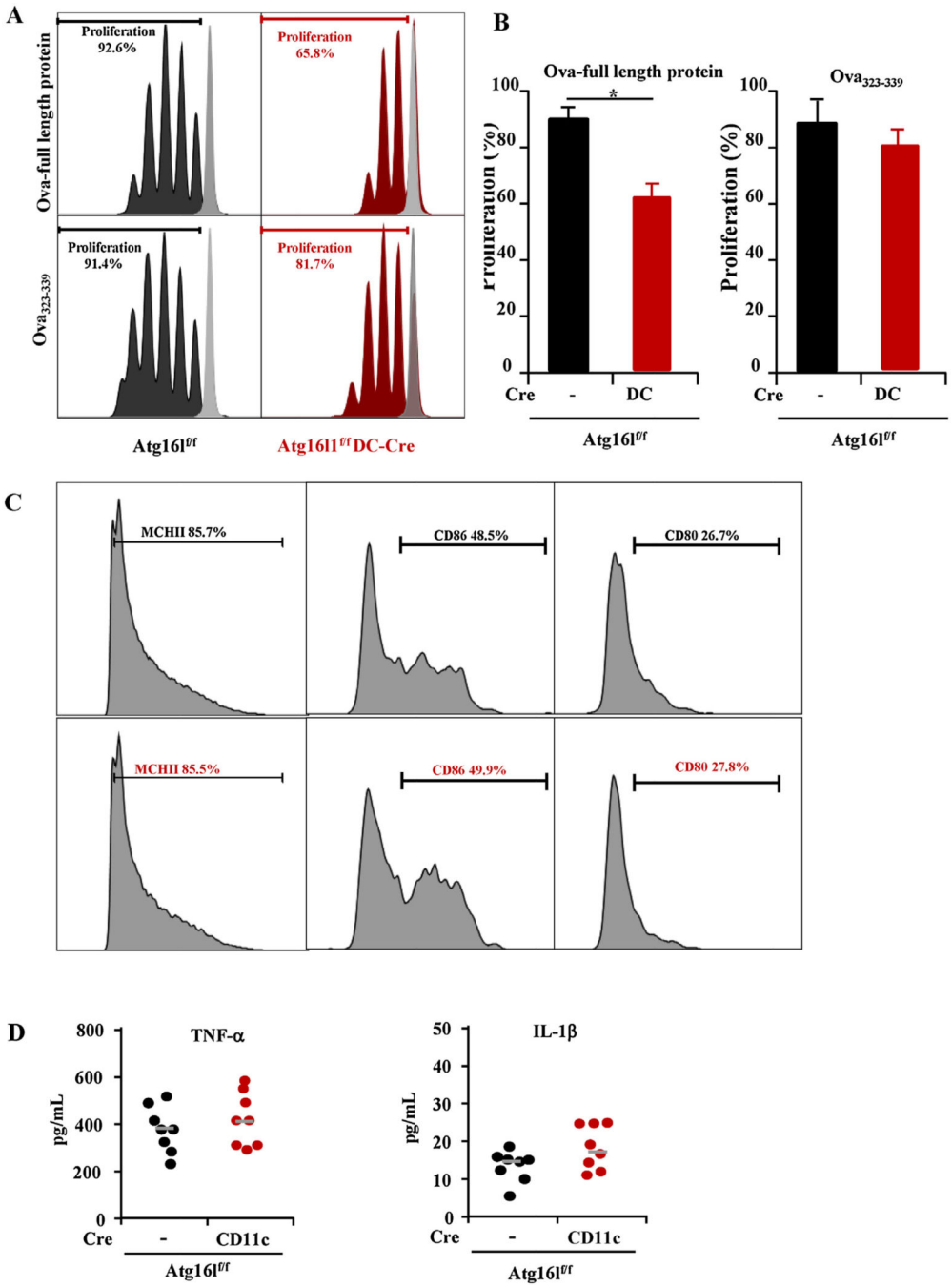

Fig. 6.

Atg16l1 is required for optimal antigen processing by BMDCs for MHCII antigen presentation. (A) Representative flow cytometry plots of proliferating OT-II CD4$^+$ T cells labeled with Cell Trace stimulated with BMM treated with whole Ova protein or Ova peptide 323–339 are shown. (B) Decreased Cell Trace fluorescence intensity indicated proliferation. (C) The expressions of MCHII, CD86 and CD80 on the BMDCs from Atg16l1$^{f/f}$ and Atg16l1ΔDC mice upon LPS stimulation. (D) The production of TNF-α and

IL-1β in BMDCs of Atg16l1$^{f/f}$ and Atg16l1ΔDC mice upon LPS stimulation. (n = 8, *P < 0.05).